

## Development and optimization of a binding assay for the XIAP BIR3 domain using fluorescence polarization

Zaneta Nikolovska-Coleska,<sup>a</sup> Renxiao Wang,<sup>a</sup> Xueliang Fang,<sup>a</sup> Hongguang Pan,<sup>b</sup> York Tomita,<sup>b</sup> Peng Li,<sup>c</sup> Peter P. Roller,<sup>c</sup> Krzysztof Krajewski,<sup>c</sup> Naoyuki G. Saito,<sup>d</sup> Jeanne A. Stuckey,<sup>e</sup> and Shaomeng Wang<sup>a,\*</sup>

<sup>a</sup> University of Michigan Comprehensive Cancer Center, Departments of Internal Medicine and Medicinal Chemistry, University of Michigan, 1500 E. Medical Center Drive, Ann Arbor, MI 48109-0934, USA

<sup>b</sup> Lombardi Cancer Center, Georgetown University Medical Center, W213 Research Building, 3970 Reservoir Road NW, Washington, DC 20057-1469, USA

<sup>c</sup> Laboratory of Medicinal Chemistry, National Cancer Institute, FCRDC, Bldg 376, Frederick, MD 21702-1201, USA

<sup>d</sup> Department of Radiation Oncology, University of Michigan, Ann Arbor, MI 48109, USA

<sup>e</sup> Life Sciences Institute, University of Michigan, Ann Arbor, MI 48109, USA

Received 24 February 2004

Available online 20 July 2004

### Abstract

The X-linked inhibitor of apoptosis protein (XIAP) is a potent cellular inhibitor of apoptosis. Designing small-molecule inhibitors that target the BIR3 domain of XIAP, where Smac/DIABLO (second mitochondria-derived activator of caspase/direct IAP-binding protein with low pI) and caspase-9 bind, is a promising strategy for inhibiting the antiapoptotic activity of XIAP and for overcoming apoptosis resistance of cancer cells mediated by XIAP. Herein, we report the development of a homogeneous high-throughput assay based on fluorescence polarization for measuring the binding affinities of small-molecule inhibitors to the BIR3 domain of XIAP. Among four fluorescent probes tested, a mutated N-terminal Smac peptide (AbuRPFK-(5-Fam)-NH<sub>2</sub>) showed the highest affinity ( $K_d = 17.92$  nM) and a large dynamic range ( $\Delta mP = 231 \pm 0.9$ ), and was selected as the most suitable probe for the binding assay. The binding conditions (DMSO tolerance and stability) have been investigated. Under optimized conditions, a  $Z'$  factor of 0.88 was achieved in a 96-well format for high-throughput screening. It was found that the popular Cheng–Prusoff equation is invalid for the calculation of the competitive inhibition constants ( $K_i$  values) for inhibitors in the FP-based competitive binding assay conditions, and accordingly, a new mathematical equation was developed, validated, and used to compute the  $K_i$  values. An associated Web-based computer program was also developed for this task. Several known Smac peptides with high and low affinities have been evaluated under the assay conditions and the results obtained indicated that the FP-based competitive binding assay performs correctly as designed: it can quantitatively and accurately determine the binding affinities of Smac-based peptide inhibitors with a wide range of affinities, and is suitable for high-throughput screening of inhibitors binding to the XIAP BIR3 domain.

© 2004 Elsevier Inc. All rights reserved.

**Keywords:** Apoptosis; XIAP; Smac/DIABLO; Fluorescence polarization assay; High-throughput screening; Cheng–Prusoff equation; Mathematical model;  $K_i$  calculation

Apoptosis, or programmed cell death, is a critical process in both development and homeostasis of multicellular organisms [1]. Alterations in apoptotic pathways can disrupt the delicate balance between cell proliferation and cell death and lead to a variety of diseases [2].

\* Corresponding author. Fax: 1-734-647-9647.

E-mail address: [shaomeng@umich.edu](mailto:shaomeng@umich.edu) (S. Wang).

Inhibitors of apoptosis proteins (IAPs)<sup>1</sup> are an important class of endogenous cellular inhibitors of apoptosis [3,4]. Among all the IAPs identified to date, human X-linked IAP (XIAP) is the most potent inhibitor of apoptosis [3] and has a key inhibitory function in both intrinsic and extrinsic apoptosis pathways [5]. XIAP functions as a potent apoptosis inhibitor by binding to and inhibiting an initiator caspase-9 and two effector caspases (caspase-3 and 7) [6–9].

XIAP contains three BIR domains as well as a C-terminal RING finger, and these domains exhibit distinct specificities for caspases [10]. Structure-function analysis of XIAP has shown that the third BIR domain (BIR3) selectively inhibits caspase-9, while the linker region between BIR1 and BIR2 inhibits caspase-3 and -7 [7,9,11,12]. The interaction between XIAP and caspases can be inhibited by a second mitochondrial activator of caspases/direct IAP-binding protein (Smac/DIABLO), a polypeptide released from mitochondria upon initiation of the apoptotic signaling process [13–16]. Structural and biological studies have demonstrated that the XIAP-Smac binding involves a well-defined surface groove in the BIR3 domain and four amino acid residues (AVPI or Ala-Val-Pro-Ile) at the N-terminus of Smac [14,16]. This four-residue binding motif, known as the IAP-binding motif (IBM) is also present in human and mouse caspase-9, *Drosophila* proteins Grim, Hid, and Reaper, which also bind to IAPs [17].

XIAP and other IAPs are overexpressed in multiple human cancer tissues and cancer cell lines and their expression levels are associated with resistance to apoptosis [18–20]. Several studies have demonstrated that XIAP plays a critical role in the resistance of cancer cells to chemotherapeutic agents, radiation, and the death ligand Apo-2L/TRAIL (tumor necrosis factor- $\alpha$ -related apoptosis-inducing ligand) [21–23]. Different approaches have recently been explored for inhibiting the antiapoptotic function of XIAP. These include antisense oligonucleotides [24] and small-molecule inhibitors of XIAP [25–27].

We are particularly interested in the discovery and design of small-molecule inhibitors of XIAP which target its BIR3 domain because this domain plays a critical role in the inhibition of apoptosis: (1) It binds to caspase-9, traps caspase-9 in a monomeric inactive form,

and potentially inhibits caspase-9-mediated apoptosis. (2) It binds to Smac protein and inhibits the proapoptotic activity of Smac protein. Thus, small-molecule inhibitors that bind to the BIR3 domain of XIAP can increase the sensitivity of cells to apoptotic stimuli through promotion of the activation of caspase-9 and the proapoptotic activity of Smac protein.

One of the essential elements in discovering and identifying small-molecule inhibitors of XIAP is the development of a robust, quantitative, and high-throughput assay for evaluation of the binding affinities of potential small-molecule inhibitors. Fluorescence polarization (FP) is a sensitive, homogeneous high-throughput method that has been exploited for both protein binding and enzymatic reactions [28–32]. FP-based assay was employed for determination of the binding affinities of Smac peptides to both the BIR2 and the BIR3 domains of XIAP [14], and more recently a high-throughput assay was reported for screening small-molecules that bind to the BIR3 domain of XIAP [26]. Our laboratory has recently reported the discovery and characterization of a naturally occurring quinone, embelin, as a fairly potent, cell-permeable small-molecule inhibitor that binds to the XIAP BIR3 domain [27].

Herein we describe our further development and optimization of the FP-based binding assay for the XIAP BIR3 domain through synthesis and evaluation of several fluorescent tracers. Furthermore, we found that the popular Cheng-Prusoff equation is invalid for the calculation of the competitive inhibition constants ( $K_i$  values) for inhibitors in the FP-based competitive binding assay conditions. Accordingly, a new mathematical equation was developed and validated for computing the  $K_i$  values, and an associated Web-based computer program was also developed for this task and is freely available to other researchers.

## Materials and methods

### *Expression and purification of XIAP BIR3 domain*

The recombinant BIR3 domain (residues 241–356) of human XIAP protein fused to His-tag (pET28b, Novagen) was overexpressed from *Escherichia coli* BL21(DE3) cells (Novagen) grown in LB medium. When the cell density reached  $OD_{600} \sim 0.8$ , the protein expression was induced by addition of isopropyl- $\beta$ -D-thiogalactopyranoside (IPTG) to a final concentration of 1 mM and zinc acetate to 100  $\mu$ M for 3 h at 37 °C. Collected cells were treated with lysozyme at a final concentration of 100  $\mu$ g/ml for 15 min at room temperature in 50 mM Tris-HCl, pH 7.5, 200 mM NaCl, and lysed by ultrasonication (Sonicator 3000 with a microprobe, Misonix) at 4 °C. Most of the protein was found in the soluble fraction and was purified using TALON

<sup>1</sup> Abbreviations used: IAPs, inhibitor of apoptosis protein; XIAP, X-linked inhibitor of apoptosis protein; BIR domain, baculovirus IAP repeat; Smac/DIABLO, second mitochondria-derived activator of caspase/direct IAP-binding protein with low pI; IBM, IAP-binding motif; FP, fluorescence polarization; HTS, high-throughput screening; Abu, L-2-aminobutyric acid; DCM, dichloromethane; DIEA, diisopropylethylamine; DMSO, dimethyl sulfoxide; EDT, ethanedithiol; HATU, O-(7-azabenzotriazol-1-yl)-N,N,N',N'-tetramethyluronium hexafluorophosphate; HOAt, 1-hydroxy-7-aza-benzotriazole; IPTG, isopropyl- $\beta$ -D-thiogalactopyranoside; NMP, N-methylpyrrolidine; PAL, 5-(4-aminomethyl-3,5-dimethoxyphenoxy)valeric acid resin; TFA, trifluoroacetic acid; TIS, triisopropyl silane.

(Clontech) or Ni-NTA (Qiagen) affinity chromatography, HiTrap Q XL (Amersham Biosciences), followed by G75 size-exclusion chromatography (Amersham Biosciences) using an FPLC system (AKTA purifier-10, Amersham Biosciences). The purified protein was stored in 50 mM Tris-HCl, pH 8.0, 300 mM KCl, 50  $\mu$ M zinc acetate, and 1 mM DTT at 4 °C.

#### Synthesis of Smac peptides

The peptides utilized in this paper, and listed in Table 3, were synthesized on an ABI 433A peptide synthesizer, starting the synthesis with PAL or Rink amide resins, to establish the C-terminal carboxamide terminal, or with Fmoc-Glu(O-t-Bu)-Wang resin, to establish the C-terminal carboxylic acid (peptide **1**), and using synthesis protocols based on standard Fmoc chemistry. The N-termini of peptides were unprotected. The resin-anchored peptide was cleaved from the resin and simultaneously deprotected by TFA-containing scavengers. The crude products were purified by reverse-phase HPLC with a water/acetonitrile gradient containing 0.05% TFA. Structures were confirmed by mass spectrometry, using an FAB mass spectrometer (VG 7070E-HF) and/or a MALDI-TOF mass spectrometer (Kratos/Shimadzu). All peptides were >95% pure, based on their HPLC analysis and mass spectral data.

#### Synthesis of the lysine side-chain fluorescent-labeled peptides

Four fluorescent labeled peptides (Table 1) with two different fluorescent markers, 6-(fluorescein-5(6)-carboxamido)hexanoic acid (Flu) or 5-carboxyfluorescein (5-Fam), were synthesized, following two different procedures.

Two peptides with Flu fluorescent marker, the N-terminal Smac nonapeptide (AVPIAQKSE-K(Flu)-OH) (**1F**) and the heptapeptide (ARPFAQK(Flu)-NH<sub>2</sub>) (**2F**), were synthesized according to the following procedure. First, Fmoc-Lys(Alloc)-OH was attached to a PAL amide resin (this step was omitted in the synthesis of **1F** using an Fmoc-Lys(Alloc)-Wang resin). Then the requisite 6 additional amino acids were attached using standard peptide synthesis protocols. The N-terminal alanine was first protected with a Boc protective group. Next, the protected peptide was treated with Pd[P(Ph)<sub>3</sub>]<sub>4</sub>

in order to selectively remove the Alloc protective group from the lysine side chain of the peptide. The resulting peptide was treated with 6-(fluorescein-5(6)-carboxamido)hexanoic acid *N*-succinimidyl ester, in the presence of diisopropylethylamine (DIEA). Finally, the peptide was removed from the resin, and simultaneously side-chain deprotected with TFA containing 2.5% EDT, 5% thioanisole, and 5% H<sub>2</sub>O at RT for 2 h.

The other two peptides with 5-Fam fluorescent marker, AbuRPFAQ-K(5-Fam)-NH<sub>2</sub> (**3F**) and AbuRPF-K(5-Fam)-NH<sub>2</sub> (**4F**), were synthesized according to the following procedure. First, Fmoc-Lys(Mtt)-OH was attached to a Rink amide resin, followed by attachment of six additional Fmoc-amino acids, using standard peptide synthesis protocols. Next, the fully protected peptide on the resin was treated with 1% TFA in DCM in order to selectively remove the Mtt protective group from the lysine side chain. The resulting peptide on the resin was mixed for 2 h with a solution of 5-carboxyfluorescein, HATU, HOAt, and DIEA in NMP, and then washed with DCM and methanol. Finally, the peptide was removed from the resin and simultaneously side-chain deprotected with TFA, containing 2.5% TIS and 2.5% H<sub>2</sub>O at room temperature, for 2 h. After HPLC purification, the molecular weights were confirmed by mass spectra (Kratos/Shimadzu MALDI-TOF mass spectrometer). The purity of all fluorescent peptides was over 95%, based on their HPLC and mass spectra analysis.

#### Determination of the fluorescent peptides/XIAP equilibrium dissociation constant ( $K_d$ )

Fluorescence polarization experiments were performed in Dynex 96-well, black, round-bottom plates (Fisher Scientific) using the Ultra plate reader (Tecan U.S., Research Triangle Park, NC). To each well, fluorescein-labeled Smac peptides (5 nM) and increasing concentrations of XIAP-BIR3 domain protein (from 0 to 40  $\mu$ M) were added to a final volume of 125  $\mu$ l in the assay buffer (100 mM potassium phosphate, pH 7.5; 100  $\mu$ g/ml bovine  $\gamma$ -globulin; 0.02% sodium azide, purchased from Invitrogen, Life Technologies). The plate was mixed on a shaker for 15 min and incubated at room temperature for 3 h to reach equilibrium. The polarization values in millipolarization units (mP) were measured at an excitation wavelength at 485 nm and an emission wavelength at 530 nm. For assay stability

Table 1

Four fluorescent peptides evaluated in XIAP polarization assays, their  $K_d$  values, and maximum dynamic binding ranges

Fluorescent peptides	Amino acid sequence	$K_d$ (nM)	Dynamic range ( $\Delta$ mP)
<b>1F</b>	AVPIAQKSE-K(Flu)-OH	244.7	234 $\pm$ 7
<b>2F</b>	ARPFAQ-K(Flu)-NH <sub>2</sub>	38.4	230 $\pm$ 4
<b>3F</b>	AbuRPFAQ-K(5-Fam)-NH <sub>2</sub>	77.6	275 $\pm$ 5
<b>4F</b>	AbuRPF-K(5-Fam)-NH <sub>2</sub>	17.9	255 $\pm$ 4

testing, a plate was measured at different times over a 24-h period. To determine the effect of DMSO on the assay, binding experiments were performed under conditions similar to those described above except that the amount of DMSO was varied. An equilibrium binding isotherm was constructed by plotting the FP reading as a function of the XIAP BIR3 protein concentration at a fixed concentration of a probe. All experimental data were analyzed using Prism 3.0 software (Graphpad Software, San Diego, CA) and the inhibition constants were determined by nonlinear curve fitting as the concentration of the XIAP BIR3 protein at which 50% of the ligand is bound.

#### Competitive binding experiments

The corresponding unlabeled peptides, together with several other peptides, were tested for their ability to displace the **4F** fluorescent probe from XIAP BIR3. Negative controls containing XIAP BIR3 and probe (equivalent to 0% inhibition), and positive controls containing only free **4F** peptide (equivalent to 100% inhibition), were included on each assay plate.

The dose-dependent binding experiments were carried out with serial dilutions of peptides, prepared in DMSO. A 5- $\mu$ l sample of the tested samples and preincubated XIAP BIR3 protein (0.030  $\mu$ M) and **4F** peptide (0.005  $\mu$ M) in the assay buffer were added in 96-well plates to produce a final volume of 125  $\mu$ l. The polarization values were measured after a 3-h incubation.  $IC_{50}$  values were determined from the plot using nonlinear least-squares analysis. The  $K_i$  values of competitive inhibitors were calculated using the newly derived equation described in this paper, based upon the measured  $IC_{50}$  values, the  $K_d$  value of the probe and XIAP BIR3 complex, and the concentrations of the protein and probe in the competition assay.

#### High-throughput assay and data calculations

To evaluate the quality and suitability of the XIAP-BIR3 fluorescence polarization assay for high-throughput screening, we determined the  $Z'$  factor, which is an indicator of the viability of the assay for screening by incorporating the precision of an assay [33],

$$Z' = 1 - \frac{(3SD_f + 3SD_b)}{(\mu_b - \mu_f)}$$

where  $SD_f$  and  $SD_b$  are the standard deviation of the signal (mP) for free and bound probe, respectively,  $\mu_b$  represents the mean of the signal obtained for the bound probe in the absence of a competitive inhibitor, and  $\mu_f$  is the mean of the free probe in the absence of the XIAP BIR3 protein (0% bound). To monitor the robustness and reproducibility of the 96-well high-throughput format, the means of both free and bound peptide probes

from each assay plate were obtained and analyzed by a scatter plot.

## Results and discussion

#### Determination of the binding affinity $K_d$ of synthetic fluorescent peptides

Smac/DIABLO was identified as one of the proapoptotic proteins translocated from mitochondria to cytosol in response to apoptotic stimuli. Full-length mature Smac protein and several peptides with different lengths, as well as mutant peptides, have been tested for their binding affinity to the BIR3 domain of XIAP. In fact, a nonapeptide (AVPIAQKSE) derived from the Smac N-terminus and the tetrameric AVPI peptide have the same binding affinity ( $K_d = 0.43$  and  $0.48 \mu$ M, respectively) to the XIAP-BIR3 as the mature Smac protein ( $K_d = 0.42 \mu$ M) [14,34]. Recently, a mutated Smac tetrapeptide (ARPF) was shown to have a higher binding affinity ( $K_d = 0.02 \mu$ M) to the XIAP BIR3 domain than that of the natural Smac AVPI peptide ( $K_d = 0.48 \mu$ M) [34]. It was also determined that mutations of the first amino acid residue (Ala1) in general greatly diminished the binding affinities, but a slight enhancement in binding affinity was observed with the unnatural amino acid, L-2-aminobutyric acid (AbuVPI) ( $K_d = 0.24 \mu$ M). These interactions between the XIAP BIR3 and the Smac peptides form the basis for development of a fluorescence polarization assay.

We have synthesized four different fluorescent probes using fluorescein as a fluorophore (Table 1): the N-terminal Smac peptide with sequence AVPIAQKSEK(Flu)-OH termed **1F**; the mutated heptapeptide (ARPFQAQK(Flu)-NH<sub>2</sub>), **2F**, where valine at position 2 and isoleucine at position 4 were mutated to arginine and phenylalanine, respectively; mutated heptapeptide, (AbuRPFQAQK(5-Fam)-NH<sub>2</sub>), termed **3F** where we have made an additional mutation at position 1 with unnatural amino acid, L-2-aminobutyric acid (Abu), and the same mutated peptide, but a shorter pentameric (AbuRPFK(5-Fam)-NH<sub>2</sub>), termed **4F**.

These four fluorescent probes were first tested in a saturation binding experiment to determine their binding affinity to XIAP BIR3 domain (Fig. 1). The initial testing conditions were based on several criteria. Since the polarization value is derived from the ratio of bound versus free probe, we chose a low concentration of probe which would yield a reasonable fluorescent signal and therefore a stable polarization value. The concentration of all tested probes was 5 nM, significantly lower than the anticipated  $K_d$ , but adequate to give enough relative fluorescence units to provide a good signal-to-noise ratio. The dissociation constant ( $K_d$ ) for each protein/ligand pair was determined using a constant concentration of

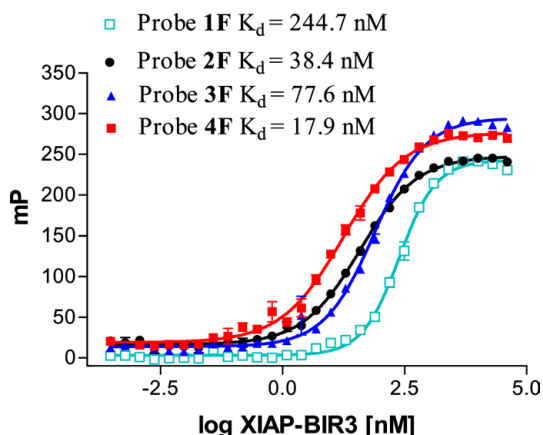


Fig. 1. Binding isotherms of fluorescent Smac peptides to XIAP/BIR3 domain. All probes in concentrations of 5 nM with increasing concentrations of XIAP-BIR3 domain (from 0 to 40  $\mu$ M) were added to a final volume of 125  $\mu$ l in the assay buffer (100 mM potassium phosphate, pH 7.5; 100  $\mu$ g/ml bovine  $\gamma$ -globulin; 0.02% sodium azide). Probe **1F**, AVPIAQKSE-K(Flu)-OH; Probe **2F** ARPFAQ-K(Flu)-NH<sub>2</sub>; Probe **3F** AbuRPFQK-K(5-Fam)-NH<sub>2</sub>; Probe **4F** AbuRPF-K(5-Fam)-NH<sub>2</sub>.

probe and titrating with the XIAP/BIR3 domain protein at increasing concentrations significantly above the expected  $K_d$  of the protein-probe pair. Fig. 1 illustrates nonlinear least-squares fits to a single-site binding model for a saturation experiment in which the XIAP/BIR3 concentration varied from 0 to 40  $\mu$ M at constant probe concentration. All the tested probes showed binding and the FP values of the peptides increased as a function of XIAP/BIR3 protein concentration. The obtained  $K_d$  values and the dynamic ranges for all the tested probes were comparable to each other. The  $K_d$  of binding between the **1F** probe and the XIAP-BIR3 domain was determined to be 244.7 nM, with dynamic range ( $\Delta$ mP = mP of bound peptide – mP of free peptide) of  $234 \pm 7$  mP (Table 1). The second probe **2F** (AR-PFAQK(Flu)-NH<sub>2</sub>), in which the valine at position 2 was changed to an arginine residue and isoleucine at position 4 was changed to phenylalanine, showed a 6 times higher binding affinity than the N-terminal Smac 9-mer peptide (**1F**), with a  $K_d$  of 38.4 nM and a dynamic range of  $230 \pm 4$  mP. The value obtained is similar to the reported value for  $K_d$  of corresponding tetrapeptide ARPF [34]. The same peptide with one additional mutation at position 1 with the unnatural amino acid, L-2-aminobutyric acid, **3F**, has also shown a high binding affinity ( $K_d = 77.6$  nM) and a dynamic range of  $275 \pm 5$  mP. The  $K_d$  value obtained is slightly higher than that of the **2F** probe, with an alanine in position 1. The fourth probe, **4F**, shows the highest affinity for XIAP BIR3 protein with a  $K_d$  value of 17.9 nM. This probe also has a large dynamic range ( $255 \pm 4$  mP). Interestingly, the pentapeptide **4F** has a binding affinity 4 times better than the longer corresponding heptapeptide **3F** (17.9 nM vs 77.6 nM). Consistent with an earlier report [34], the **4F** probe has a binding affinity 2 times better than the **2F** probe.

We have further explored if there is a change in  $K_d$  values when the concentration of the probe is reduced. In principle, when the probe concentration is above the true  $K_d$  value, a higher probe concentration will result in a higher apparent  $K_d$  value [35]. Accordingly, in the determination of the  $K_d$  value for the probe in the titration experiment, the concentration of the probe should be well below the true  $K_d$  value. Under three concentrations of probe **4F** (5, 2.5, and 1 nM), we obtained 17.9, 16.4, and 22.1 nM, respectively, as the apparent  $K_d$  values for **4F** probe. Our results thus indicated that the apparent  $K_d$  value for the probe obtained under each of the three concentrations approaches the true  $K_d$  value.

We have tested the influence of DMSO, a commonly used solvent, in high-throughput screening in the presence of either 4 or 8% DMSO. The results obtained showed that the binding affinity of **4F** probe is unchanged in the presence of DMSO; the dynamic range and the shape of the binding curve were not altered, indicating that the FP assay is stable in the presence of up to 8% DMSO.

The stability of the XIAP FP assay is critical for high-throughput screening and has been tested by incubating the plate at room temperature over a 24-h period, reading the plate several times, and analyzing the data. The results obtained showed that the assay is stable, as evidenced by the binding curves (Fig. 2). The obtained  $K_d$  values and the binding ranges remained unchanged.

#### Development and optimization of the competitive binding assay

Based on the information obtained in saturation experiments, the  $K_d$  values and dynamic binding ranges, each of these fluorescent peptide probes is suitable for development of an FP-based assay. Indeed, the **1F** probe

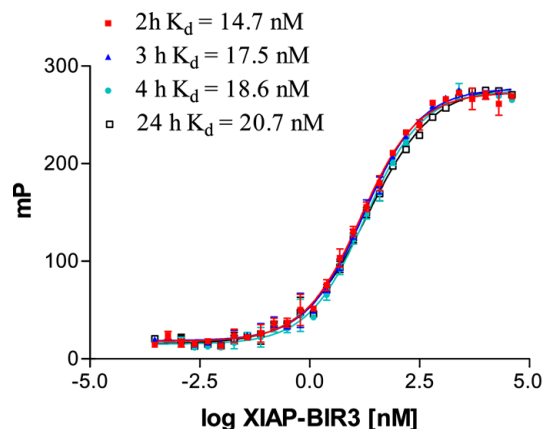


Fig. 2. Stability of binding experiments over a 24-h period. Binding experiments were performed using 5 nM **4F** probe and increasing concentrations of XIAP BIR3 protein (from 0 to 40  $\mu$ M). The plate was measured at the specified time indicated over the experimental period.

Table 2  
 $IC_{50}$  and  $K_i$  values of several unlabeled Smac peptides using different conditions in FP-based competitive assay

Concentration of XIAP BIR3 (nM)	Tested peptides								
	AVPIAQKSE-OH (1)			ARPFQKS-NH <sub>2</sub> (2)			AbuRPFK-NH <sub>2</sub> (4)		
	Measured $IC_{50}$ ( $\mu$ M)	$K_i$ ( $\mu$ M) Cheng's equation	$K_i$ ( $\mu$ M) New equation	Measured $IC_{50}$ ( $\mu$ M)	$K_i$ ( $\mu$ M) Cheng's equation	$K_i$ ( $\mu$ M) New equation	Measured $IC_{50}$ ( $\mu$ M)	$K_i$ ( $\mu$ M) Cheng's equation	$K_i$ ( $\mu$ M) New equation
30	1.16	0.91	0.43	0.24	0.19	0.081	0.22	0.17	0.074
60	2.52	2.0	0.57	0.40	0.31	0.082	0.39	0.31	0.079
120	3.10	2.43	0.40	0.73	0.57	0.082	0.77	0.60	0.088
240	8.10	6.33	0.55	1.81	1.41	0.11	1.58	1.24	0.095

was previously used for the FP-based XIAP-binding assay [14]. A mutated Smac N-terminal heptapeptide (AVPFAQK-(Flu)-NH<sub>2</sub>) was also used for the development of an FP-based binding assay and for identification of novel small-molecule inhibitors of the XIAP BIR3 domain [26]. Using the **2F** as the probe, we have established an FP-based competitive binding assay and reported the discovery of Embelin as a novel nonpeptidic small-molecule inhibitor of XIAP [27]. To increase the sensitivity and the detection limit of the assay, we have further optimized the FP-based assay by synthesizing new fluorescent probes, **3F** and **4F**. We have selected **4F** as the probe for further development and optimization of the FP-based assay for the XIAP BIR3 domain based on the following considerations: (i) high binding affinity ( $K_d = 17.92$  nM) which will allow us to increase the detection limit of the assay and (ii) large dynamic range ( $255 \pm 4$  mP) which will give better signal-to-noise ratio.

The concentrations of the tracer and the protein used in the FP-based assay need to be carefully chosen to maximize the difference between the highest and lowest polarization values and to increase the sensitivity of the assay. FP competition experiments should be designed in such a way that the  $[receptor]/K_d$  ratio is at least 1, and the starting polarization value represents approximately 50% of the maximal FP change observed in the saturation experiment [37].

We have shown that the **4F** probe has similar apparent  $K_d$  values (17.9, 16.4, and 22.1 nM) in all three tested concentrations (2.5, 1, and 5 nM, respectively). Recently it was demonstrated that with increased concentrations of the fluorescent tracer in the assay, the interference from fluorescent compounds is reduced [38]. Because the influence of fluorescent compounds depends on the concentration of the probe used in the assay, we have chosen to use 5 nM for the probe. This concentration of the probe has high fluorescence intensity and can overcome the potential interference of any weakly fluorescent compounds.

To determine the optimal concentration of the protein, we have evaluated four different concentrations of the XIAP BIR3 domain (30, 60, 120, and 240 nM) with a

fixed concentration of **4F** (5 nM) in the competitive binding assay to determine the  $IC_{50}$  of three corresponding unlabeled peptides: N-terminal Smac 9-mer peptide **1**, and two mutated Smac peptides **2** and **4** (Table 2). The lowest protein concentration was chosen based on the fact that 30 nM XIAP is about 1.5 times the actual  $K_d$  value of the tracer and at this concentration a majority of the fluorescent probe will be bound to the protein. At 30 nM XIAP, the assay yielded  $88 \pm 2.43$  mP as the dynamic range (Fig. 3). As expected, using 60 nM (3 times the  $K_d$ ), 120 nM (6 times the  $K_d$ ), and 240 nM (12 times the  $K_d$ ) as the protein concentration, the dynamic range of the assay was increased to 121, 180, and 220 mP, respectively (Fig. 3). With higher protein concentrations, the obtained  $IC_{50}$  values of the competitors were increased. There is a good correlation between the observed  $IC_{50}$  values and concentrations of the protein used in the assay (Table 2). The obtained  $IC_{50}$  values for these peptides are significantly higher than the  $K_d$  values of corresponding fluorescent labeled peptide tracers, but the rank order is the same under all the conditions. Based on these results, we chose to use 30 nM XIAP/BIR3 protein for the competitive binding assay. This assay

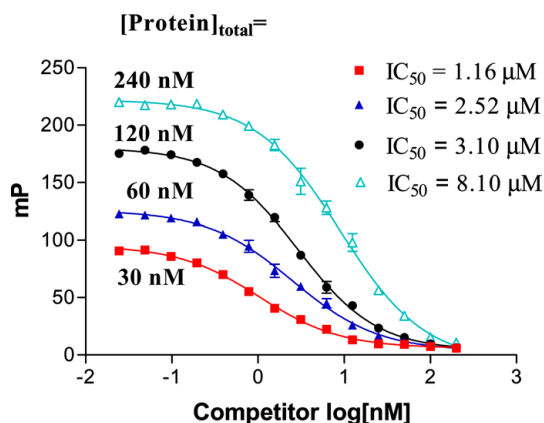


Fig. 3. Displacement of **4F** probe (AbuRPF-K(5-Fam)-NH<sub>2</sub>) from XIAP/BIR3 domain by N-terminal Smac 9-mer peptide (AVPIAQKSE-OH, **1**), using four protein concentrations. Increasing protein concentration increases the dynamic range of the assay but also increases the  $IC_{50}$ .

condition uses a relatively low concentration of the protein but yields a quite large dynamic range, and is sensitive and suitable for high-throughput screening.

*Advantages of using a high-affinity probe for the development of an FP-based assay*

Recently, it was shown [36] that in FP competition assays, there is a general misconception that a tightly binding fluorescent probe should be avoided when identifying inhibitors of low or intermediate potency in the screening of small-molecule compound libraries. However, it was demonstrated that the higher the affinity of the fluorescent ligand, the wider the range of inhibitor potency that can be resolved [36]. The lowest inhibitor  $K_i$  value that can be resolved in an FP-based binding assay is approximately equal to the  $K_d$  value of the fluorescent probe [36]. To demonstrate the relationship between the  $IC_{50}$  of inhibitors and the  $K_d$  values of the fluorescent ligand used in the assay, we have determined the binding affinity of three tetrapeptides with a large difference in their inhibitory potencies, using two fluorescent probes, **1F** and **4F**, which have 14-time differences in their  $K_d$  values (244.7 and 17.9 nM, respec-

tively). As can be seen from Fig. 4, for every tetrapeptide the obtained  $IC_{50}$  values are higher when **1F** was used as the probe than those when **4F** was used as the probe. Furthermore, for a weak inhibitor such as AVPR tetrapeptide, the difference in their  $IC_{50}$  values obtained using either **1F** or **4F** (Fig. 4A) is only 2-fold. For a potent inhibitor such as the ARPF tetrapeptide, the difference in their  $IC_{50}$  values obtained using either **1F** or **4F** (Fig. 4A) is increased to 5-fold (Fig. 4C). Hence, our results demonstrate that using a high-affinity probe **4F**, we can accurately measure the binding affinity of highly potent compounds to XIAP BIR3 by increasing the assay detection limit.

There are considerable advantages to using **4F** as the probe in the FP-based XIAP assay compared to previously used probes with weaker affinities [14,26]. First, the use of this high-affinity probe increases in the assay sensitivity and detection limit, so that the binding affinities of potent inhibitors can be accurately measured. Second, the use of this high-affinity probe significantly decreases the amount of the XIAP/BIR3 protein needed in the binding assays, which makes high-throughput screening cheaper without compromising the assay sensitivity and accuracy.

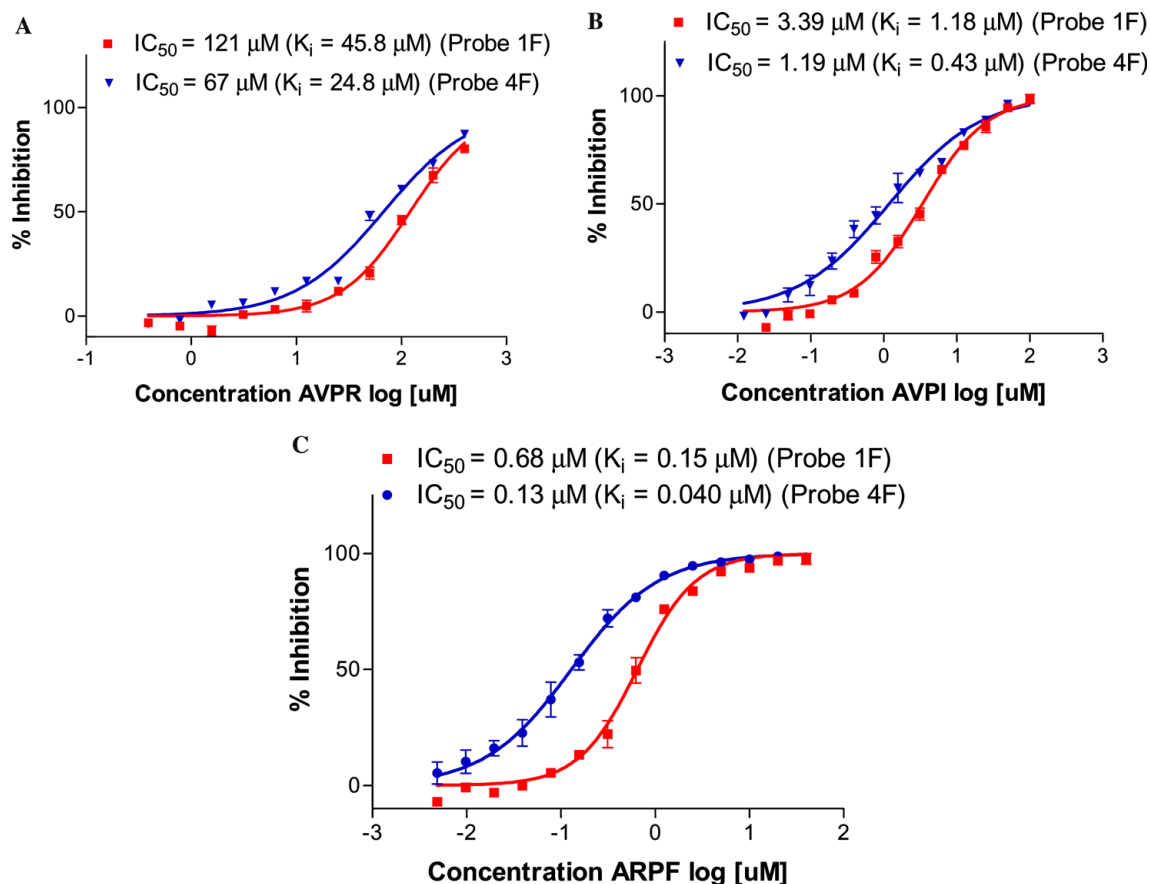


Fig. 4. Competitive inhibition binding curves of three tetrapeptides obtained with two fluorescent probes **1F** and **4F**, which have different binding affinities to BIR3 domain ( $K_d = 245$  nM and  $K_d = 17.9$  nM, respectively), using a fixed probe concentration of 5 nM. Tested peptides: (A) AVPR-NH<sub>2</sub>; (B) AVPI-NH<sub>2</sub>; (C) ARPF-NH<sub>2</sub>.

### Validation of the competitive FP-based XIAP-binding assay

To validate the optimized FP-based competitive binding assay conditions and the new equation for calculation of  $K_i$  values, we have tested a set of natural and mutated Smac tetra-peptides with a wide range of binding affinities to the XIAP BIR3 domain protein. The results are summarized in Table 3, together with previously reported binding affinities for these peptides [34]. Of note, the  $K_i$  values for these peptides were computed using Eq. (3) in this paper. As expected, the ARPF peptide has the highest affinity ( $K_i = 0.044 \pm 0.007 \mu\text{M}$ ), followed by the AVPF peptide ( $K_i = 0.093 \pm 0.01 \mu\text{M}$ ). Two peptides (AVPIAQKSE and AVPI), derived from the Smac protein sequence, have similar binding affinities ( $K_i = 0.54 \pm 0.15$  and  $0.58 \pm 0.15 \mu\text{M}$ , respectively). Two mutated Smac peptides (AVPD and AVPR) have weak binding affinities ( $K_i = 12.34 \pm 0.39$  and  $29.09 \pm 1.88 \mu\text{M}$ , respectively). The  $K_i$  values of these peptides to the XIAP BIR3 protein and their rank order (ARPF > AVPF > AVPIAQKSE > AVPI > AVPD > AVPR) are consistent with the results obtained by another method [34]. These validation experiments provide evidence that the FP competitive binding assay

can quantitatively and accurately determine the binding affinities of small-molecule inhibitors with a wide range of binding affinities to the XIAP BIR3 protein.

### High-throughput screening format

One potential use of a homogeneous and competitive assay for the XIAP BIR3 domain is to carry out high-throughput screening of chemical libraries of small organic molecules to discover inhibitors of XIAP. The FP-based assay is suitable for high-throughput screening because it requires a limited number of steps and can easily be automated. One of the parameters for determining the quality of a high-throughput assay is the  $Z'$  factor, a statistical parameter that assesses the performance of HTS assays [33]. The  $Z'$  factor is reflective of both the assay dynamic range and the data variation. Assays with small  $Z'$  factors are not suitable for high-throughput screening and require further optimization, while assays with  $Z'$  factors close to the maximum value of 1 are of high quality.

We used 5 nM of the tracer **4F** and 30 nM of the XIAP BIR3 protein in the competitive assay for high-throughput screening purpose. In Fig. 5 we present the scatter plot for the means of free and bound peptide controls from each individual assay plate. In the 96-well assay format, the  $Z'$  factor for the FP-based XIAP BIR3 competitive binding assay is found to be 0.88, thus confirming that our assay conditions are adequate for high-throughput screening.

### Development and validation of a new mathematical equation for the calculation of $K_i$ values for FP-based assays

The  $\text{IC}_{50}$  value of an inhibitor depends upon the experimental conditions, so it is often difficult to compare

Table 3

Experimental  $K_i$  values as determined by FP-based competition assay for natural and mutated Smac peptides

Peptides	$K_i \pm \text{SD}$ ( $\mu\text{M}$ )	$K_d$ ( $\mu\text{M}$ ) [34]
AVPIAQKSE-OH (1)	$0.54 \pm 0.15$	0.40
AVPI-NH <sub>2</sub> (4)	$0.58 \pm 0.15$	0.48
AVPF-NH <sub>2</sub> (5)	$0.093 \pm 0.1$	0.04
AVPD-NH <sub>2</sub> (6)	$12.34 \pm 0.39$	7.3
AVPR-NH <sub>2</sub> (7)	$29.09 \pm 1.88$	>100
ARPF-NH <sub>2</sub> (8)	$0.044 \pm 0.007$	0.02

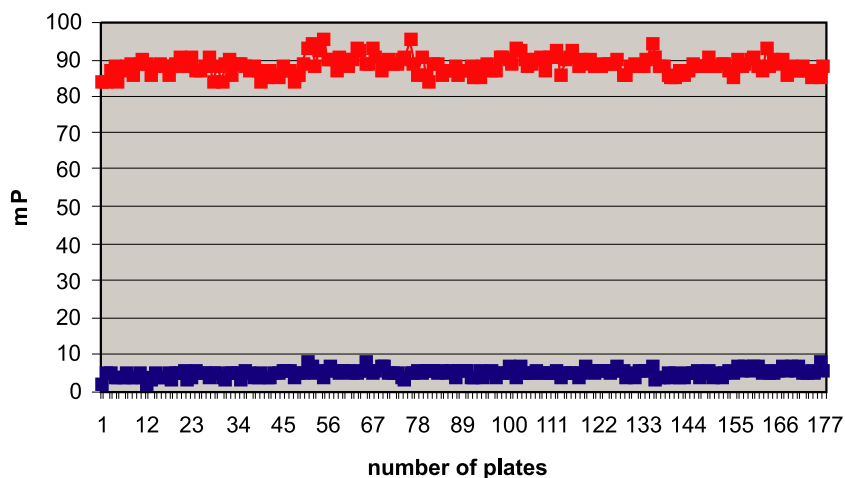


Fig. 5. Stability of free peptide control and bound peptide control from a series of 96-well assay plates. The average mP values from free peptide control (blue squares) and bound peptide control (red squares) were obtained from each assay plate. (For interpretation of the references to colour in this figure legend, the reader is referred to the web version of this paper.)

the  $IC_{50}$  values measured under different experimental conditions and from different laboratories. For this reason, a common and desirable practice is to convert the measured  $IC_{50}$  values into the inhibition constants ( $K_i$ ), which is the equilibrium constant and theoretically does not depend on the experimental conditions except the temperature.

For competitive binding assays, the Cheng–Prusoff equation [39] is widely used to compute  $K_i$  values from  $IC_{50}$  values. Although originally derived in the context of competitive inhibition of a Michaelis enzymatic reaction, the Cheng–Prusoff equation has been generalized into the following form to calculate the inhibition constants ( $K_i$  values) in receptor–ligand binding assays,

$$K_i = IC_{50}/(1 + [L]/K_d), \quad (1)$$

where  $K_i$  is the inhibition constant of an inhibitor to the receptor (protein),  $IC_{50}$  is the inhibitor concentration required to competitively dissociate 50% of the reference ligand (probe) from the receptor,  $[L]$  is the concentration of the *free* (unbound) reference ligand, and  $K_d$  is the dissociation constant between the receptor and the reference ligand. Note that the  $IC_{50}$  value in Eq. (1) is actually the concentration of the *free* inhibitor when 50% inhibition of the protein–ligand binding is established. Since this value cannot be directly measured in an FP-based competitive binding assay, normally it is replaced by the total concentration of the inhibitor when applying the Cheng–Prusoff equation. An exact correction to the Cheng–Prusoff equation, however, has been reported previously to solve this problem [40].

We found that the basic assumptions made in the derivation of the Cheng–Prusoff equation are not applicable to the FP-based binding assay conditions. First, the Cheng–Prusoff equation requires the concentration of the unbound reference ligand for computation, which cannot be measured directly in an FP-based competitive binding assay. Thus, a normal practice when applying the Cheng–Prusoff equation is to use the total concentration of the reference ligand,  $[L]_T$ , instead of the concentration of the unbound reference ligand,  $[L]$ . When  $[L]_T$  is well above the level of  $K_d$ , this approximation will not introduce a significant error, which is the case in traditional competitive binding assays where the receptor concentration is well below the ligand concentration. In a typical FP-binding assay, however, the labeled ligand (probe) is kept at a low concentration with an excess amount of protein. As discussed above, the FP assay conditions are designed to maximize the dynamic range of the mP signal. Typically, the amount of probe used in the FP-based assay is kept below the  $K_d$  value and the amount of the receptor is equal to or higher than the  $K_d$  value so that the polarization value before adding an inhibitor is at 50% or more of the maximal mP shift. Under such conditions, a significant fraction of the probe is bound to the receptor, and the free probe

concentration cannot be approximated to the total probe concentration any more. The second reason appears to be even more critical. As demonstrated in our FP-binding assay, use of higher concentrations of the receptor in the binding assay resulted in higher  $IC_{50}$  values for the same inhibitor (Fig. 3 and Table 2). However, the Cheng–Prusoff equation does not give a clue why the total concentration of the protein should have a significant impact on the  $IC_{50}$  value. Our work has demonstrated that applying the Cheng–Prusoff equation in our FP-based assay will yield higher  $K_i$  values for the same inhibitor when higher total concentrations of protein are used in the experiments (Table 2).

Kenakin provided an equation in his book [35], which can be rearranged as

$$K_i = ([I] \times [PL] \times K_d) / \{([L]_T \times [P]_T) + [PL] \times ([PL] - [P]_T - [L]_T - K_d)\}, \quad (2)$$

in which  $[I]$  denotes the concentration of the free inhibitor in the system, while  $[PL]$  is the concentration of the bound ligand, i.e., the protein–ligand complex, in the same system. Thus, if the above two properties are known, Eq. (2) can be applied to compute the  $K_i$  value of a given inhibitor in a competitive binding assay. The major advantage of this equation is that in principle it is applicable to any assay conditions regardless of the concentrations of the protein and the labeled ligand used in the binding assay. In contrast to the Cheng–Prusoff equation, Eq. (2) can provide a consistent  $K_i$  value for the same inhibitor under different protein and ligand concentrations. However, one will need the concentration of the bound ligand and the concentration of the *free* inhibitor at 50% inhibition in order to convert an  $IC_{50}$  value measured in a binding assay into  $K_i$ . Kenakin did not provide the solution of these two properties since his equation was derived from a general scenario of a competitive binding assay.

We have thus independently developed a new equation to compute the  $K_i$  values for inhibitors in FP-based binding assays. This equation is written as

$$K_i = [I]_{50} / ([L]_{50}/K_d + [P]_0/K_d + 1), \quad (3)$$

where  $[I]_{50}$  denotes the concentration of the free inhibitor at 50% inhibition,  $[L]_{50}$  is the concentration of the free labeled ligand at 50% inhibition,  $[P]_0$  is the concentration of the free protein at 0% inhibition, and  $K_d$  is the dissociation constant of the protein–ligand complex. This equation was derived from the basic principles of a competitive binding assay, as described in detail in the Appendix A. The application of Eq. (3) is not restricted by the concentrations of the protein and the ligand. Compared to Kenakin's equation, Eq. (3) is more concise.

For the purpose of accurately computing the  $K_i$  values of inhibitors using Eq. (3), we also derived the

solutions of all of the parameters required in Eq. (3). Thus, one does not need to approximate any of these values when applying Eq. (3). For the convenience of other researchers, we have implemented this equation in a CGI program, which can be freely accessed at [http://sw16.im.med.umich.edu/software/calc\\_ki/](http://sw16.im.med.umich.edu/software/calc_ki/). The user only needs to input the necessary parameters of the FP-based binding assay, i.e., the total concentration of the protein, the total concentration of the ligand (probe), the  $K_d$  value of the protein-ligand complex, and the  $IC_{50}$  value observed for a given inhibitor, and then the program will compute the  $K_i$  value of the given inhibitor accordingly.

To validate this new equation, we have applied it to the calculation of the  $K_i$  values for three Smac peptides (Table 2). As shown, regardless of the protein concentrations used in the FP-based binding assay, the computed  $K_i$  values for the same inhibitor are highly consistent with each other (Table 2), indicating that the computed  $K_i$  value for the same inhibitor is independent of the protein concentrations, as would be expected.

## Conclusions

We have established a fluorescence-polarization-based assay to evaluate small-molecule inhibitors that target the XIAP BIR3 domain where Smac and caspase-9 proteins bind. Development of assays to measure protein-protein interactions using the technique of fluorescence polarization requires careful selection of the fluorescent probes. Two main considerations are the binding affinity of the probe to the protein and the polarization signal window. A newly designed fluorescent probe (**4F**) was selected for the competitive binding assay for its high affinity ( $K_d = 17.92$  nM) and a large maximal polarization window upon its binding to the XIAP BIR3 domain protein. We demonstrated that the new competitive binding assay condition can accurately determine the binding affinities of natural and mutated Smac peptides with a wide range of binding affinities to the XIAP BIR3 domain protein, and the results are consistent with those reported previously using another method. The assay is fast and robust and performs well in the presence of DMSO. Furthermore, the assay can be adapted to a miniaturized assay format for rapid screening of large numbers of compounds to identify small-molecule inhibitors of XIAP.

To compute the binding affinity constants ( $K_i$  values) of inhibitors, we found that the FP-based competitive binding assay conditions fail to meet the basic assumptions made in the popular Cheng–Prusoff equation. Accordingly, we have derived a new mathematical equation for computing the  $K_i$  values of inhibitors from the basic principles of competitive binding assays and developed an associated web-based computer program for this task.

Using Smac peptides, we have shown that although the  $IC_{50}$  values obtained for an inhibitor in the FP-based competitive binding assay clearly depend upon experimental conditions such as the protein concentration, the calculated  $K_i$  values for the inhibitor are independent of the experimental conditions, as one would expect, for the  $K_i$  value is a thermodynamic property.

## Acknowledgments

We greatly appreciate the financial support from the Susan G. Komen Foundation, the CapCure Foundation (now the Prostate Cancer Foundation), the Department of Defense Prostate Cancer Program, and the National Institutes of Health (to S.W.). We thank Dr. George W.A. Milne for his critical reading of the manuscript. The web-based computer program for computing  $K_i$  values is public accessible at [http://sw16.im.med.umich.edu/software/calc\\_ki/](http://sw16.im.med.umich.edu/software/calc_ki/).

## Appendix A

This section describes the derivation of an equation that computes the inhibition constant ( $K_i$ ) of a competitive inhibitor from its  $IC_{50}$  value observed in a fluorescence polarization (FP)-based competitive binding assay. This equation is derived from the basic principles of competitive binding assay, which are in principle generally applicable to FP-based competitive binding assays regardless of the concentration ranges of the protein and the labeled ligand.

### A.1. The basic principles in a competitive binding assay

Let  $P$  denote for the protein molecule,  $L$  for the fluorescence-labeled ligand molecule,  $I$  for the competitive inhibitor,  $PL$  for the protein-ligand complex, and  $PI$  for the protein-inhibitor complex. Here we assume that  $I$  inhibits the binding of  $L$  to  $P$  in a competitive way, and both  $L$  and  $I$  bind to  $P$  with a stoichiometry of 1:1. Let  $[P]$ ,  $[L]$ ,  $[I]$ ,  $[PL]$ , and  $[PI]$  denote for the concentrations of these five species, respectively, and  $[P]_T$ ,  $[L]_T$ , and  $[I]_T$  denote for the total concentration of the protein, the ligand, and the inhibitor, respectively. In a competitive binding assay, at any time,

$$[P]_T = [P] + [PL] + [PI] \quad (\text{A.1})$$

$$[L]_T = [L] + [PL] \quad (\text{A.2})$$

$$[I]_T = [I] + [PI]. \quad (\text{A.3})$$

Let  $K_d$  denote the dissociation constant of the  $PL$  complex and  $K_i$  the dissociation constant of the  $PI$  complex. When the system reaches equilibrium

$$K_d = [P][L]/[PL] \quad (\text{A.4})$$

$$K_i = [P][I]/[PI]. \quad (\text{A.5})$$

### A.2. The theorem of 50% inhibition in an FP-based binding assay

Let us assume that the FP signal detected at any time is determined by the ratio of the bound labeled ligand,  $[PL]$ , and the free labeled ligand,  $[L]$ , in a linear manner,

$$FP = C_{PL} \times ([PL]/[L]_T) + C_L \times ([L]/[L]_T) \\ = (C_{PL} - C_L) \times ([PL]/[L]_T) + C_L, \quad (\text{A.6})$$

where  $C_{PL}$  and  $C_L$  are the coefficients of  $PL$  and  $L$  for FP signal, respectively. In an FP-based binding assay, a positive control, in which the protein usually is mixed with the labeled ligand in an amount of  $[P]_T$  and  $[L]_T$ , defines the maximal level of the FP signal ( $FP_{\max}$ ), while a negative control, which has labeled ligand alone in an amount of  $[L]_T$ , defines the minimal level of FP signal ( $FP_{\min}$ ). For the positive control, i.e., 0% inhibition, by applying Eq. (A.6) one has

$$FP_{\max} = FP_0 = (C_{PL} - C_L) \times [PL]_0/[L]_T + C_L. \quad (\text{A.6.1})$$

For the negative control, i.e., 100% inhibition, one has

$$FP_{\min} = FP_{100} = C_L. \quad (\text{A.6.2})$$

Similarly, when 50% inhibition is observed in an FP-based binding assay:

$$FP_{50} = (C_{PL} - C_L) \times [PL]_{50}/[L]_T + C_L. \quad (\text{A.6.3})$$

In an FP-based binding assay, the inhibition ratio at any point on the inhibition curve is defined as

$$\text{Inhibition}\% = 1 - (FP - FP_{\min})/(FP_{\max} - FP_{\min}) \quad (\text{A.7})$$

From the above equation, when 50% inhibition is achieved:

$$FP_{50} = (FP_0 + FP_{100})/2. \quad (\text{A.8})$$

Substitute Eqs. (A.6.1), (A.6.2) and (A.6.3) into this equation and simplify it, and one has

$$[PL]_{50} = 1/2 \times [PL]_0, \quad (\text{A.9})$$

where  $[PL]_{50}$  is the concentration of  $PL$  when 50% inhibition is achieved;  $[PL]_0$  is the concentration of  $PL$  without  $I$  in the system, i.e., 0% inhibition or positive control. Eq. (A.9) is the fundamental theorem when 50% inhibition is observed in an FP-based competitive binding assay.

### A.3. The equation for computing $K_i$ from $IC_{50}$ observed in an FP-based binding assay

Based on Eq. (A.9), one can derive an equation for computing the  $K_i$  value of  $I$  from the  $IC_{50}$  value. When  $I$  is not in the system, one has, from Eqs. (A.1) and (A.4):

$$[PL]_0 = [P]_T/(1 + K_d/[L]_0). \quad (\text{A.10})$$

When  $I$  is added to the system, one has, from Eqs. (A.1), (A.4) and (A.5):

$$[PL] = [P]_T/\{1 + (K_d/[L]) \times (1 + [I]/K_i)\}. \quad (\text{A.11})$$

Substitute Eqs. (A.10) and (A.11) into Eq. (A.9),

$$1 + (K_d/[L]_{50}) \times (1 + [I]_{50}/K_i) = 2 \times (1 + K_d/[L]_0),$$

which can be rearranged to

$$K_i = [I]_{50}/([L]_{50}/K_d + 2 \times [L]_{50}/[L]_0 - 1) \quad (\text{A.12})$$

and

$$K_i = [I]_{50}/([L]_{50}/K_d + 2 \times ([L]_{50} - [L]_0)/[L]_0 + 1) \\ = [I]_{50}/([L]_{50}/K_d + 2 \times \{([L]_T - [PL]_{50}) \\ - ([L]_T - [PL]_0)\}/[L]_0 + 1) \\ = [I]_{50}/([L]_{50}/K_d + 2 \times ([PL]_0 - [PL]_{50})/[L]_0 + 1)$$

Combining this with Eq. (A.9):

$$K_i = [I]_{50}/([L]_{50}/K_d + [PL]_0/[L]_0 + 1) \\ = [I]_{50}/([L]_{50}/K_d + [P]_0/K_d + 1). \quad (\text{A.13})$$

Eq. (A.13) shows how the  $K_i$  value can be accurately computed if the concentration of the free inhibitor at 50% inhibition,  $[I]_{50}$ , the concentration of the free labeled ligand at 50% inhibition,  $[L]_{50}$ , and the concentration of the free protein at 0% inhibition,  $[P]_0$ , and the dissociation constant of the protein-ligand complex,  $K_d$ , are known. This is the equation we have used in our study to compute  $K_i$  values.

### A.4. Solution of Eq. (A.13)

The properties required to apply Eq. (A.13), i.e.,  $[I]_{50}$ ,  $[L]_{50}$ , and  $[P]_0$ , can be computed as follows:

#### A.4.1. Solution of the 0% inhibition point

At this point, there are only  $P$  and  $L$  in the system.  $[L]_0$ ,  $[P]_0$ , and  $[PL]_0$  can be solved analytically with given  $[P]_T$ ,  $[L]_T$ , and  $K_d$ . From Eqs. (A.1) and (A.5), one has

$$[P]_0 = [P]_T/(1 + [L]_0/K_d).$$

From Eqs. (A.2) and (A.5), one has

$$[L]_0 = [L]_T/(1 + [P]_0/K_d).$$

Combining the above two equations and simplifying the result gives

$$[P]_0^2 + (K_d + [L]_T) \times [P]_0 - [P]_T = 0.$$

The correct value of  $[P]_0$  is the positive root of the above quadratic equation. Once  $[P]_0$  is solved,  $[L]_0$  and  $[PL]_0$  can be derived easily with Eqs. (A.1) and (A.2).

#### A.4.2. Solution of the 50% inhibition point

As indicated in Eq. (A.9),  $[PL]_{50}$  can be computed directly from  $[PL]_0$ :

$$[PL]_{50} = [PL]_0/2.$$

Consequently,  $[L]_{50}$  can be computed through Eq. (A.2):

$$[L]_{50} = [L]_T - [PL]_{50} = [L]_T - [PL]_0/2.$$

Also,  $[I]_{50}$  can be computed through Eqs. (A.3) and (A.1):

$$\begin{aligned} [I]_{50} &= IC_{50} - [PI]_{50} \\ &= IC_{50} - ([P]_T - [P]_{50} - [PL]_{50}) \\ &= IC_{50} - [P]_T + K_d \times [PL]_{50}/[L]_{50} + [PL]_{50}. \end{aligned}$$

With known  $[I]_{50}$ ,  $[L]_{50}$ , and  $[P]_0$ ,  $K_i$  can be computed accurately with Eq. (A.13).

## References

- [1] G.S. Salvesen, C.S. Duckett, IAP proteins: blocking the road to death's door, *Nature Rev. Mol. Cell Biol.* 3 (2002) 401–410.
- [2] J.C. Reed, Apoptosis-based therapies, *Nature Rev. Drug Discov.* 1 (2002) 111–121.
- [3] Q.L. Deveraux, J.C. Reed, IAP family proteins—suppressors of apoptosis, *Genes Dev.* 13 (1999) 239–252.
- [4] E.C. LaCasse, S. Baird, R.G. Korneluk, A.E. MacKenzie, The inhibitors of apoptosis (IAPs) and their emerging role in cancer, *Oncogene* 17 (1998) 3247–3259.
- [5] S.W. Fesik, Insights into programmed cell death through structural biology, *Cell* 103 (2000) 273–282.
- [6] R. Takahashi, Q. Deveraux, I. Tamm, K. Welsh, N. Assa-Munt, G.S. Salvesen, J.C. Reed, A single BIR domain of XIAP sufficient for inhibiting caspases, *J. Biol. Chem.* 273 (1998) 7787–7790.
- [7] S.J. Riedl, M. Renatus, R. Schwarzenbacher, Q. Zhou, C. Sun, S.W. Fesik, R.C. Liddington, G.S. Salvesen, Structural basis for the inhibition of caspase-3 by XIAP, *Cell* 104 (2001) 791–800.
- [8] J. Chai, E. Shiozaki, S.M. Srinivasula, Q. Wu, P. Datta, E.S. Alnemri, Y. Shi, Structural basis of caspase-7 inhibition by XIAP, *Cell* 104 (2001) 769–780.
- [9] Y. Huang, Y.C. Park, R.L. Rich, D. Segal, D.G. Myska, H. Wu, Structural basis of caspase inhibition by XIAP: differential roles of the linker versus the BIR domain, *Cell* 104 (2001) 781–790.
- [10] Q.L. Deveraux, E. Leo, H.R. Stennicke, K. Welsh, G.S. Salvesen, J.C. Reed, Cleavage of human inhibitor of apoptosis protein XIAP results in fragments with distinct specificities for caspases, *EMBO J.* 18 (1999) 5242–5251.
- [11] S.M. Srinivasula, R. Hegde, A. Saleh, P. Datta, E. Shiozaki, J. Chai, R.A. Lee, P.D. Robbins, T. Fernandes-Alnemri, Y. Shi, E.S. Alnemri, A conserved XIAP-interaction motif in caspase-9 and Smac/DIABLO regulates caspase activity and apoptosis, *Nature* 410 (2001) 112–116.
- [12] C. Sun, M. Cai, R.P. Meadows, N. Xu, A.H. Gunasekera, J. Herrmann, J.C. Wu, S.W. Fesik, NMR structure and mutagenesis of the third Bir domain of the inhibitor of apoptosis protein XIAP, *J. Biol. Chem.* 275 (2000) 33777–33781.
- [13] J. Chai, C. Du, J.W. Wu, S. Kyin, X. Wang, Y. Shi, Structural and biochemical basis of apoptotic activation by Smac/DIABLO, *Nature* 406 (2000) 855–862.
- [14] Z. Liu, C. Sun, E.T. Olejniczak, R.P. Meadows, S.F. Betz, T. Oost, J. Herrmann, J.C. Wu, S.W. Fesik, Structural basis for binding of Smac/DIABLO to the XIAP BIR3 domain, *Nature* 408 (2000) 1004–1008.
- [15] S.M. Srinivasula, P. Datta, X.J. Fan, T. Fernandes-Alnemri, Z. Huang, E.S. Alnemri, Molecular determinants of the caspase-promoting activity of Smac/DIABLO and its role in the death receptor pathway, *J. Biol. Chem.* 275 (2000) 36152–36157.
- [16] G. Wu, J. Chai, T.L. Suber, J.W. Wu, C. Du, X. Wang, Y. Shi, Structural basis of IAP recognition by Smac/DIABLO, *Nature* 408 (2000) 1008–1012.
- [17] J.W. Wu, A.E. Cocina, J. Chai, B.A. Hay, Y. Shi, Structural analysis of a functional DIAP1 fragment bound to grim and hid peptides, *Mol. Cell* 8 (2001) 95–104.
- [18] G. Ambrosini, C. Adida, D.C. Altieri, A novel anti-apoptosis gene, survivin, expressed in cancer and lymphoma, *Nature Med.* 3 (1997) 917–921.
- [19] D. Vucic, H.R. Stennicke, M.T. Pisabarro, G.S. Salvesen, V.M. Dixit, ML-IAP, a novel inhibitor of apoptosis that is preferentially expressed in human melanomas, *Curr. Biol.* 10 (2000) 1359–1366.
- [20] I. Tamm, S.M. Kornblau, H. Segall, S. Krajewski, K. Welsh, S. Kitada, D.A. Scudiero, G. Tudor, Y.H. Qui, A. Monks, M. Andreeff, J.C. Reed, Expression and prognostic significance of IAP-family genes in human cancers and myeloid leukemias, *Clin. Cancer Res.* 6 (2000) 1796–1803.
- [21] M. Holcik, C. Yeh, R.G. Korneluk, T. Chow, Translational upregulation of X-linked inhibitor of apoptosis (XIAP) increases resistance to radiation induced cell death, *Oncogene* 19 (2000) 4174–4177.
- [22] H. Sasaki, Y. Sheng, F. Kotsuji, B.K. Tsang, Down-regulation of X-linked inhibitor of apoptosis protein induces apoptosis in chemoresistant human ovarian cancer cells, *Cancer Res.* 60 (2000) 5659–5666.
- [23] C.P. Ng, B. Bonavida, X-linked inhibitor of apoptosis (XIAP) blocks Apo2 ligand/tumor necrosis factor-related apoptosis-inducing ligand-mediated apoptosis of prostate cancer cells in the presence of mitochondrial activation: sensitization by overexpression of second mitochondria-derived activator of caspase/direct IAP-binding protein with low pl (Smac/DIABLO), *Mol. Cancer Ther.* 1 (2002) 1051–1058.
- [24] Y. Hu, G. Cherton-Horvat, V. Dragowska, S. Baird, R.G. Korneluk, J.P. Durkin, L.D. Mayer, E.C. LaCasse, Antisense oligonucleotides targeting XIAP induce apoptosis and enhance chemotherapeutic activity against human lung cancer cells in vitro and in vivo, *Clin. Cancer Res.* 9 (2003) 2826–2836.
- [25] T.Y. Wu, K.W. Wagner, B. Bursulaya, P.G. Schultz, Q.L. Deveraux, Development and characterization of nonpeptidic small molecule inhibitors of the XIAP/caspase-3 interaction, *Chem. Biol.* 10 (2003) 759–767.
- [26] C.J. Glover, K. Hite, R. DeLosh, D.A. Scudiero, M.J. Fivash, L.R. Smith, R.J. Fisher, J.W. Wu, Y. Shi, R.A. Kipp, G.L. McLendon, E.A. Sausville, R.H. Shoemaker, A high-throughput screen for identification of molecular mimics of Smac/DIABLO utilizing a fluorescence polarization assay, *Anal. Biochem.* 320 (2003) 157–169.
- [27] Z. Nikolovska-Coleska, Z. Hu, L. Xu, Y. Tomita, P. Li, P.P. Roller, R. Wang, X. Fang, M.E. Lippman, M. Zhang, D. Yang, S. Wang, Discovery of embelin as a cell-permeable, small-molecular weight inhibitor of XIAP through structure-based computational screening of traditional herbal medicine three-dimensional structural database, *J. Med. Chem.* 47 (2004) 2430–2440.
- [28] P. Wu, M. Brasseur, U. Schindler, A high-throughput STAT binding assay using fluorescence polarization, *Anal. Biochem.* 249 (1997) 29–36.
- [29] S.S. Pin, I. Kariv, N.R. Graciani, K.R. Oldenburg, Analysis of protein-peptide interaction by a miniaturized fluorescence polarization assay using cyclin-dependent kinase 2/cyclin E as a model system, *Anal. Biochem.* 275 (1999) 156–161.
- [30] R. Bolger, T.E. Wiese, K. Ervin, S. Nestich, W. Checovich, Rapid screening of environmental chemicals for estrogen receptor binding capacity, *Environ. Health Perspect.* 106 (1998) 551–557.

- [31] J.C. Owicki, Fluorescence polarization and anisotropy in high throughput screening: perspectives and primer, *J. Biomol. Screen.* 5 (2000) 297–306.
- [32] A.J. Pope, U.M. Haupts, K.J. Moore, Homogeneous fluorescence readouts for miniaturized high-throughput screening: theory and practice, *Drug Discov. Today* 4 (1999) 350–362.
- [33] J.H. Zhang, T.D. Chung, K.R. Oldenburg, A simple statistical parameter for use in evaluation and validation of high throughput screening assays, *J. Biomol. Screen.* 4 (1999) 67–73.
- [34] R.A. Kipp, M.A. Case, A.D. Wist, C.M. Cresson, M. Carrell, E. Griner, A. Wiita, P.A. Albinak, J. Chai, Y. Shi, M.F. Semmelhack, G.L. McLendon, Molecular targeting of inhibitor of apoptosis proteins based on small molecule mimics of natural binding partners, *Biochemistry* 41 (2002) 7344–7349.
- [35] T. Kenakin, *Pharmacological Analysis of Drug-Receptor Interaction*, Lippincott-Raven, Philadelphia, 1997.
- [36] X. Huang, Fluorescence polarization competition assay: the range of resolvable inhibitor potency is limited by the affinity of the fluorescent ligand, *J. Biomol. Screen.* 8 (2003) 34–38.
- [37] PanVera Fluorescence Polarization Technical Resource Guide, Panvera Corporation, Madison, WI, 2002, pp.3–13.
- [38] T.C. Turek-Etienne, E.C. Small, S.C. Soh, T.A. Xin, P.V. Gaitonde, E.B. Barrabee, R.F. Hart, R.W. Bryant, Evaluation of fluorescent compound interference in 4 fluorescence polarization assays: 2 kinases, 1 protease, and 1 phosphatase, *J. Biomol. Screen.* 8 (2003) 176–184.
- [39] Y. Cheng, W.H. Prusoff, Relationship between the inhibition constant ( $K_I$ ) and the concentration of inhibitor which causes 50 per cent inhibition ( $I_{50}$ ) of an enzymatic reaction, *Biochem. Pharmacol.* 22 (1973) 3099–3108.
- [40] P.J. Munson, D. Rodbard, An exact correction to the “Cheng–Prusoff” correction, *J. Recept. Res.* 8 (1988) 533–546.